

A revised interpretation of the structure of $(\text{NH}_4)_2\text{Ge}_7\text{O}_{15}$ in the light of the Extended Zintl–Klemm Concept

 Angel Vegas^{a*} and Harry Donald Brooke Jenkins^{b,c}
^aUniversidad de Burgos, Hospital del Rey s/n, 09001 Burgos, Spain, ^bDepartment of Chemistry, University of Warwick, Coventry CV4 7AL, England, and ^c'Fieldgate', 3 White Hill, Olney, Buckinghamshire MK46 5AY, England.

*Correspondence e-mail: diegas2002@gmail.com

Received 12 October 2016

Accepted 2 December 2016

Edited by E. V. Boldyreva, Russian Academy of Sciences, Russia

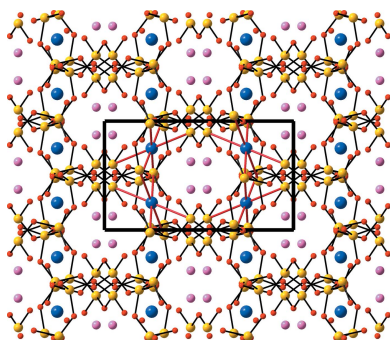
Keywords: germanates; crystal chemistry; Zintl polyanions; ionic strength.

The structure of $(\text{NH}_4)_2\text{Ge}_7\text{O}_{15}$ recently described as being a microporous material containing rings, in which GeO_6 octahedra coexist with GeO_4 tetrahedra, is re-examined in the light of the Extended Zintl–Klemm Concept as applied to cations in oxides. The $\text{Ge}^{[6]}$ atoms together with the NH_4^+ groups act as true cations, transferring their 6 valence electrons to the acceptor Ge_2O_5 moiety, so converting it into the $[\text{Ge}_6\text{O}_{15}]^{6-} \equiv 3(\Psi\text{-As}_2\text{O}_5)$ ion (where Ψ refers to a pseudo-lattice) and yielding threefold connectivity. The tetrahedral Ge network shows similarities with the Sb_2O_3 analogue. At the same time, the $\text{Ge}^{[6]}$ atoms are connected to other $\text{Ge}^{[4]}$ atoms forming blocks that are part of a rutile-type GeO_2 structure. Such an analysis shows that both substructures (the Zintl polyanion and the rutile fragments) must be satisfied simultaneously as has already been illustrated in previous articles which considered stuffed-bixbyites [Vegas *et al.* (2009). *Acta Cryst.* **B65**, 11–21] as well as the compound FeLiPO_4 [Vegas (2011). *Struct. Bond.* **138**, 67–91]. This new insight conforms well to previous (differential thermal analysis) DTA–TGA (thermogravimetric analysis) experiments [Cascales *et al.* (1998). *Angew. Chem. Int. Ed.* **37**, 129–131], which show endothermic loss of NH_3 and H_2O to give rise to the metastable structure Ge_7O_{14} , which further collapses to the rutile-type GeO_2 structure. We analyze the stability change in terms of ionic strength, I , and so provide a means of rationalizing the driving force behind this concept capable of explaining the atomic arrangements found in these types of crystal structures. Although the concept was formulated in 2003, later than the publication of the germanate structure, it was not used or else ignored by colleagues who solved this crystal structure.

1. Introduction

The synthesis and structure determination of the title compound $(\text{NH}_4)_2\text{Ge}_7\text{O}_{15}$ (see Fig. 1) was reported by Cascales *et al.* (1998). The structure was described as being formed by a three-dimensional $[\text{Ge}_7\text{O}_{15}]^{2-}$ germanate anion neutralized by ammonium cations. The authors gave special emphasis to the existence of GeO_4 (tetrahedral) and GeO_6 (octahedral) polyhedra in the nine-membered-rings forming part of this three-dimensional skeleton. However, the coexistence of both types of coordination number (CN), also found in aluminates, silicates, silicophosphates and oxonitridosilicates, remained unmentioned by the authors.

As similar examples of this coexistence of CNs we can cite sillimanite $\text{Al}^{[6]}_2[\text{Al}^{[4]}_2\text{Si}^{[4]}_2\text{O}_{10}]$ (Yang *et al.*, 1997), the high-pressure phases of $\text{Na}_2\text{Si}^{[6]}[\text{Si}^{[4]}_2\text{O}_7]$ (Fleet & Henderson, 1995), $\text{K}_2\text{Si}^{[6]}[\text{Si}^{[4]}_3\text{O}_9]$ (Swanson & Prewitt, 1983), $\text{Na}_6\text{Si}^{[6]}_3[\text{Si}^{[4]}_9\text{O}_{27}]$ (Fleet, 1996) and $\text{Na}_8\text{Si}^{[6]}[\text{Si}^{[4]}_6\text{O}_{18}]$ (Fleet, 1998). This same feature also occurs in the silicophosphates $\text{Si}^{[6]}[\text{P}^{[4]}_2\text{O}_7]$ (Bissert & Liebau, 1969) and $\text{Si}^{[6]}_3[\text{Si}^{[4]}_2\text{P}^{[4]}_6\text{O}_{25}]$



(Poojary *et al.*, 1993) under ambient pressure and the phenomenon has further been observed in the oxidonitridosilicate $\text{Ce}_{16}\text{Si}^{[6]}[\text{Si}^{[4]}_{14}\text{O}_6\text{N}_{32}]$ (Köllisch & Schnick, 1999) which, like germanate of the title, are compounds also obtained at ambient pressure.

It is well known that silicon is normally tetrahedrally coordinated and that octahedral coordination should be regarded as an abnormal feature in solid-state silicates, which has traditionally been attributed to be the result of the application of pressure. In this context the quartz \rightarrow stishovite transition has been explained and in a similar manner, and for similar reasons, the presence of hexa-coordinated silicon in the high-pressure phases of $\text{Na}_2\text{Si}^{[6]}[\text{Si}^{[4]}_2\text{O}_7]$ (Fleet & Henderson, 1995), $\text{K}_2\text{Si}^{[6]}[\text{Si}^{[4]}_3\text{O}_9]$ (Swanson & Prewitt, 1983), $\text{Na}_6\text{Si}^{[6]}_3[\text{Si}^{[4]}_9\text{O}_{27}]$ (Fleet, 1996) and $\text{Na}_8\text{Si}^{[6]}[\text{Si}^{[4]}_6\text{O}_{18}]$ (Fleet, 1998) has been attributed to this external pressure.

However, in $\text{Si}^{[6]}[\text{P}^{[4]}_2\text{O}_7]$ (Bissert & Liebau, 1969), in $\text{Si}^{[6]}_3[\text{Si}^{[4]}_2\text{P}^{[4]}_6\text{O}_{25}]$ (Poojary *et al.*, 1993) and in $\text{Ce}_{16}\text{Si}^{[6]}[\text{Si}^{[4]}_{14}\text{O}_6\text{N}_{32}]$ (Köllisch & Schnick, 1999), the Si atoms are hexa-coordinated *and these are not high-pressure phases*. The presence of $[\text{AO}_6]$ octahedra ($A = \text{Si}, \text{Ge}$) in compounds obtained at ambient pressure was an unexpected outcome in the case of silicon, but could also be more plausible in germanates.

The reason for this is that, at normal pressure, GeO_2 exists as a rutile-type structure (possessing GeO_6 octahedra; Goldschmidt, 1932) that converts into the quartz-type structure (tetra-coordinated Ge atoms) at 1305 K. In contrast, SiO_2 exists as quartz at ambient pressure but requires further application of pressure in order to achieve a CN = 6 as found

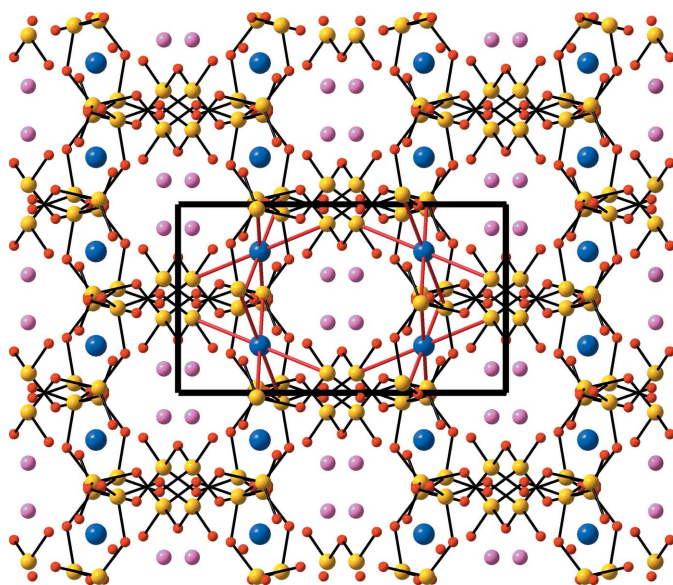


Figure 1

The structure of $(\text{NH}_4)_2\text{Ge}^{[6]}[\text{Ge}^{[4]}_6\text{O}_{15}]$ projected onto the ab plane showing the Ge–O network formed by $\text{Ge}^{[4]}$ (yellow spheres) and O atoms (small red spheres). The $\text{Ge}^{[4]}$ –O bonds are drawn with black lines. The octahedrally coordinated $\text{Ge}^{[6]}$ atoms are represented by dark blue spheres. They are linked with red lines to six $\text{Ge}^{[4]}$ atoms. Lilac spheres represent the N atoms of NH_4^+ cations. The H atoms have been omitted.

in stishovite (rutile-type; Stishov & Belov, 1962). Because the structure of $(\text{NH}_4)_2[\text{Ge}_7\text{O}_{15}]$ also contains $[\text{GeO}_4]$ and $[\text{GeO}_6]$ polyhedra, the compound can be formulated, in accordance with related silicates, as $(\text{NH}_4)_2\text{Ge}^{[6]}[\text{Ge}^{[4]}_6\text{O}_{15}]$. This structural formula indicates that only one of the seven Ge atoms per formula unit is octahedrally coordinated, whereas the other six form the anionic tetrahedral skeleton $[\text{Ge}^{[4]}_6\text{O}_{15}]^{6-}$. The complete skeleton is represented in Fig. 1 following the description of Cascales *et al.* (1998).

The two different CNs exhibited by Al, Si and Ge atoms in some compounds described above are difficult to explain if we are thinking of the existence of either Al^{3+} , Si^{4+} or Ge^{4+} isolated cations to which we can assign a given ‘ionic volume’ (Jenkins *et al.*, 1999). However, a rational insight emerges if we think of the existence (or pre-existence) of polyanions brought about by amphoteric behaviour of the p -block atoms, *i.e.* if both the electropositive cations (Na, K *etc.*) and the $[\text{A}^{[6]}]$ atoms, when acting as an acid, would donate their valence electrons to the $[\text{T}^{[4]}]$ atoms, whilst when acting as a base, the tetrahedral Si atoms would yield the $[\text{Si}_2\text{O}_7]^{6-}$, $[\text{Si}_3\text{O}_9]^{6-}$, $[\text{Si}_6\text{O}_{18}]^{12-}$, $[\text{Si}_9\text{O}_{27}]^{18-}$ anions present in the HP phases. This same feature is to be expected in the anion $[\text{Si}_{14}\text{O}_6\text{N}_{32}]^{20-}$ and also in the title germanate $[\text{Ge}^{[4]}_6\text{O}_{15}]^{6-}$. In other words, the $[\text{A}^{[6]}]$ atoms, by acting as cations, convert the $[\text{T}^{[4]}]$ atoms into anions.

Such a model arises from our extension of the Zintl–Klemm concept and has more than proved its usefulness already in rationalizing multitudinous structures of aluminates (Santamaría-Pérez & Vegas, 2003), silicates (Santamaría-Pérez *et al.*, 2005) and many other structures (Vegas, 2011, 2017). In the present article we apply this concept to the structure of $(\text{NH}_4)_2\text{Ge}^{[6]}[\text{Ge}^{[4]}_6\text{O}_{15}]$ in order to provide a rational explanation of its tetrahedral Ge-skeleton.

2. Description of the structure

In 2003, Santamaría-Pérez & Vegas proposed an extension to the Zintl–Klemm concept in order to account for the structures of the cation networks of inorganic structures. The application of this fruitful concept to the structures of both aluminates (Santamaría-Pérez & Vegas, 2003) and silicates (Santamaría-Pérez *et al.*, 2005), presented a new, coherent interpretation and rationalization of the structures of these two great families of compounds. Their previous interpretation was restricted to a classification of the different tetrahedral skeletons that were thought of as having been formed by the condensation of AlO_4 , SiO_4 or PO_4 groups. The classical book of Liebau (1985) on silicates and that of Durif (1995) on phosphates provides proof of the efforts made by numerous scientists to classify, and further understand, these apparent ‘capricious networks’ that are observed in these families of compounds. Also worthy of mention in this context are the works of Parthé and co-workers (Parthé & Engel, 1986; Parthé & Chabot, 1990) who also sought to provide a general classification of all the known types of tetrahedral structures. These authors realised that the Zintl–Klemm concept was embodied in those compounds and they tried to

explain their connectivity by applying that concept to the entire tetrahedral skeletons including both *T* and *O* atoms. However, they failed in relating the *Al* (*Si*) skeletons with pseudo-elements or pseudo-molecules as well as failing to account for the multiple CN (tetrahedral and octahedral) adopted by some elements in the same crystal. Nevertheless, the term coined by them to denote the *T* atoms (*Al* or *Si*) as ‘cations *ex-officio*’ deserves a mention because it implies the admission that the *T* atoms (*Si* or *Al*) had lost their cationic character.

One of the most important achievements which this new approach of ours brings to the table (Santamaría-Pérez & Vegas, 2003; Santamaría-Pérez *et al.*, 2005) is the rationalization of the coordination number CN adopted by silicon in its varying compounds. As explained above, in other related compounds the tetrahedral [*TO*₄] (*T* = *Al*, *Si*, *P*) groups are

found to coexist with [*AO*₆] octahedra (*A* = *Al*, *Si*). However, their coexistence was puzzling in light of the radius ratio rules and it could only be explained when the approach by Santamaría-Pérez & Vegas (2003) and Santamaría-Pérez *et al.* (2005) was applied. As was mentioned in §1, that explanation was based on the amphoteric behaviour of both *Al* and *Si* atoms.

Whilst it is true that the application of pressure can promote the donor character as well as causing an increase in the CN, pressure alone, we contend, is not always the sole cause for this to be observed. Were this so, all *Si* atoms in the high-pressure phase $\text{Na}_2\text{Si}^{[6]}[\text{Si}^{[4]}_2\text{O}_7]$ or in the ambient pressure phase $\text{Ce}_{16}\text{Si}^{[6]}[\text{Si}^{[4]}_{14}\text{O}_6\text{N}_{32}]$ would be expected to have the same CN – which they clearly do not! Thus, neither pressure effects alone, nor the effect of size, can account for this variability in the CN of silicon.

We now describe the monoclinic structure of $(\text{NH}_4)_2\text{Ge}^{[6]}[\text{Ge}^{[4]}_6\text{O}_{15}]$ by consideration, only, of the Ge-subarray, so ignoring at this stage both the *O* and the *N* atoms. The unit cell (*C*2/*c*; *Z* = 4) and its Ge partial structure is projected in Fig. 2(*a*) onto the *ac* plane. The Ge-skeleton is then seen (in Fig. 2*a*) to contain two kinds of Ge atoms: one represented with dark-blue-coloured spheres and corresponding to that forming the GeO_6 octahedra and those represented by cyan-coloured spheres which form the tetrahedral GeO_4 network. The $\text{Ge}^{[6]}$ atom (dark blue) is connected to six other $\text{Ge}^{[4]}$ atoms by means of red linkages, whereas the $\text{Ge}^{[4]}$ atoms (cyan) are interconnected by yellow linkages.

3. Two models of interpretation

The above Ge-array can be interpreted in two ways: the first one makes use of the Zintl–Klemm concept. Thus, if the $\text{Ge}^{[6]}$ and the two NH_4 groups are thought of as cations, they would transfer six electrons to the other six Ge atoms so converting them into pseudo-As atoms, $\Psi\text{-As}$. These atoms are those forming the cyan skeleton which are drawn in perspective separately in Fig. 2(*b*) where the $\text{Ge}^{[6]}$ atoms have been omitted while, inserted instead, are the *N* atoms. The purpose of this is to show that when the cations are omitted, the structure displays a three-connected

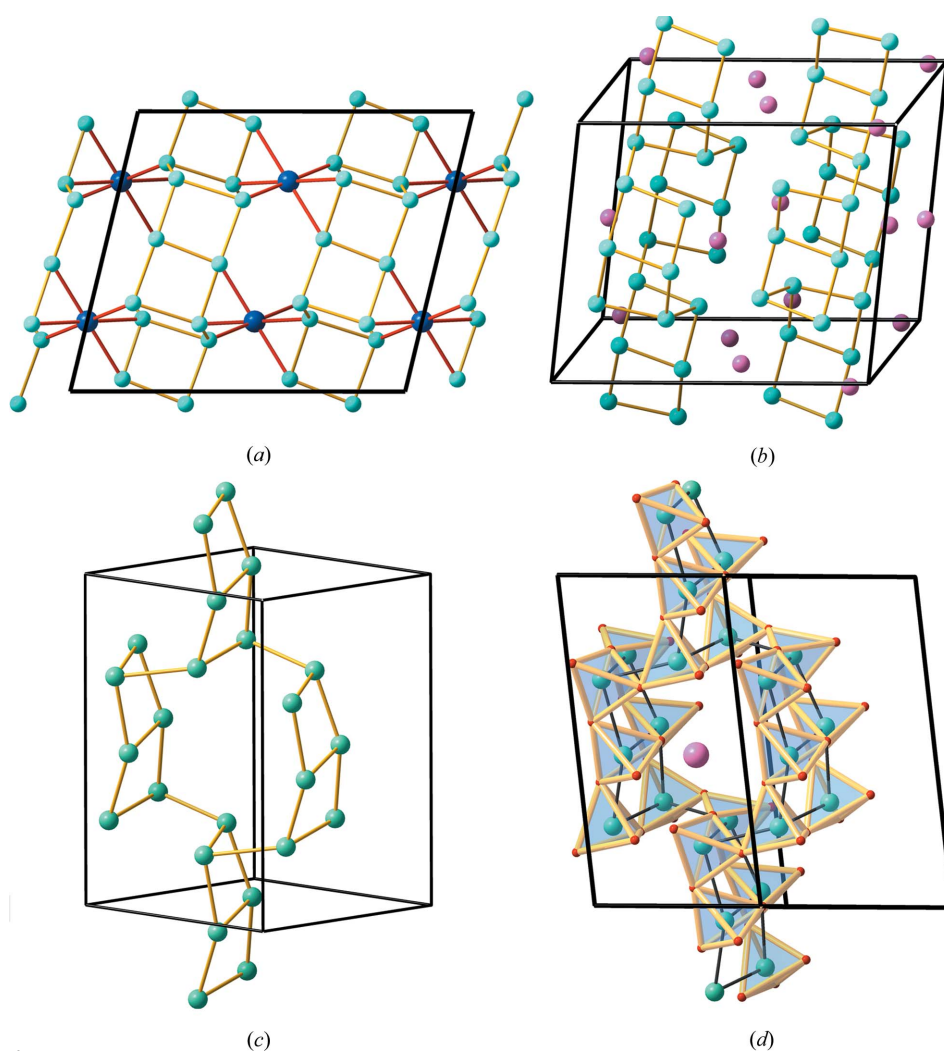


Figure 2

(*a*) The partial structure of Ge atoms in $(\text{NH}_4)_2\text{Ge}^{[6]}[\text{Ge}^{[4]}_6\text{O}_{15}]$ projected on the *ac* plane. The skeleton of $\text{Ge}^{[4]}$ atoms, with stoichiometry $[\text{Ge}_2\text{O}_5]^{2-}$, is represented by cyan spheres connected by yellow lines. The $\text{Ge}^{[6]}$ atoms, as dark blue spheres, are connected to the $\text{Ge}^{[4]}$ network by red lines. (*b*) The Ge-subarray of the tetrahedral $[\text{Ge}_2\text{O}_5]^{2-}$ network showing the threefold connectivity of the Ge atoms converted into $\Psi\text{-As}$ atoms, according to the Zintl–Klemm concept. The lilac spheres here represent the *N* atoms located in the tunnels formed by such networks. (*c*) Perspective view of one of the networks showing the tunnel where the $\text{Ge}^{[6]}$ and NH_4^+ cations reside. (*d*) The same network as in (*c*) in which the GeO_4 tetrahedra have been drawn in.

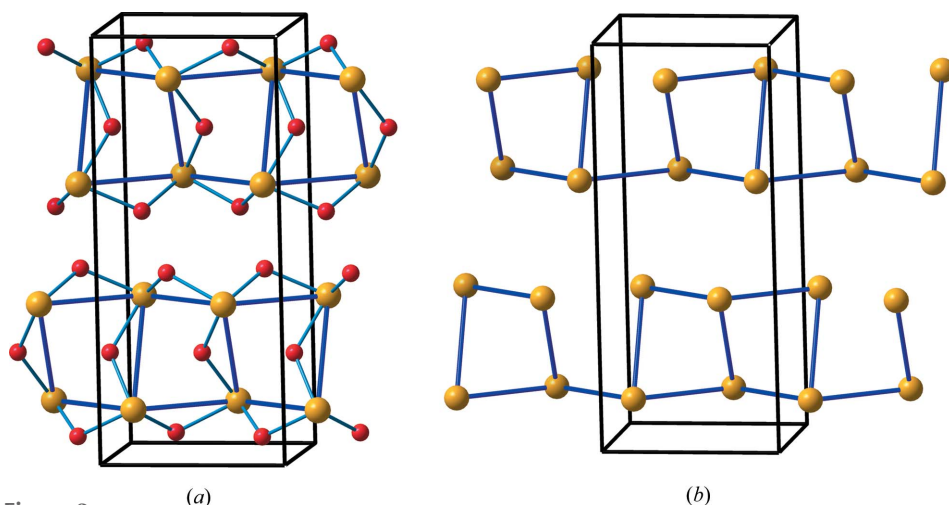


Figure 3
 (a) The structure of Sb_2O_3 ($Pccn$) exhibiting the threefold connectivity of the Sb atoms (in ochre) forming ladder-like chains from which the $\text{Ge}^{[4]}$ -skeleton of Fig. 2(b) can be derived. The O atoms (represented by small red balls) are near the centres of the Sb—Sb contacts, mimicking the hypothetical bonding pairs. The positions close to the lone pairs (LP) remain empty. Note that in the $\text{Ge}^{[4]}$ -network of Fig. 2(d) those positions are occupied so completing the GeO_4 tetrahedra. (b) The same structure without the O atoms and where some Sb—Sb bonds have been eliminated to leave pairs of rectangles like those forming the network of Fig. 2(c).

network characteristic of the elements of Group 15. This network is more easily seen in Figs. 2(c) and (d), which show the channels within which both the cations Ge^{4+} and NH_4^+ are lodged.

As has been remarked above, the six electrons provided by Ge^{4+} and NH_4^+ convert the $\text{Ge}[4]$ atoms into Ψ -As, yielding a network characteristic of the group 15 elements. The stoichiometry of that skeleton is Ge_2O_5 which is similar to the analogues P_2O_5 or As_2O_5 .

This network also has strong similarities with that of the high-temperature analogue Sb_2O_3 , the mineral valentinite ($Pccn$; Svensson, 1974), as represented in Fig. 3. In this structure the three-connected Sb atoms form ladder-like chains in which O atoms are located near to the centre of the

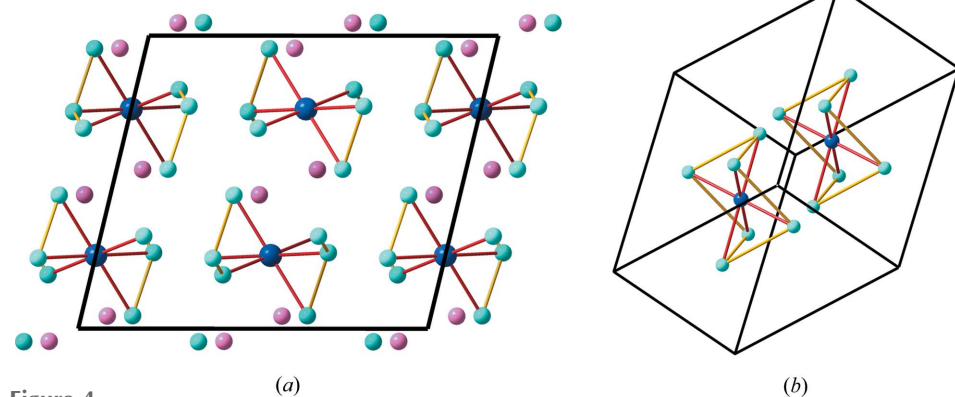


Figure 4
 (a) Projection of the structure on the ac plane, similar to that represented in Fig. 2(a). Here, some $\text{Ge}^{[4]}-\text{Ge}^{[4]}$ contacts have been eliminated giving rise to a set of isolated blocks formed by $\text{Ge}^{[6]}\text{Ge}^{[4]}_6$. Big dark blue spheres represent $\text{Ge}^{[6]}$ atoms. N atoms are represented as lilac spheres. (b) Perspective view of the two central blocks of (a). Red lines connect the $\text{Ge}^{[6]}$ atom to the six $\text{Ge}^{[4]}$ (Ψ -As) atoms. Yellow lines connect $\text{Ge}^{[4]}$ (Ψ -As) atoms.

(hypothetical) Sb—Sb bonds, which are drawn with blue lines in Fig. 3(a). If in this figure we break some Sb—Sb bonds, then we obtain pairs of pucker rectangles as represented in Fig. 3(b). These pairs of rectangles can then rotate with respect to one another so that the two-connected Sb atoms are then bonded to one Sb atom of the contiguous ladder, yielding in turn the Ψ -As skeleton of Fig. 2(c). As mentioned above, the central void serves as a cavity into which to lodge both the Ge^{4+} and NH_4^+ cations, the latter being used as templates in the synthesis of the microporous compound.

When the $[\text{Ge}_2\text{O}_5]$ partial structure is compared with the Sb_2O_3 structure, we see that their differences can be attributed to their different O content. Thus, in the $[\text{Ge}_2\text{O}_5]$ partial structure, the Ge

(Ψ -As) atoms are tetrahedrally coordinated, whereas in Sb_2O_3 the lower O content leads to a CN = 3, so creating vacancies close to the expected LP positions (Fig. 3a).

A second approach to the interpretation of the structure of $(\text{NH}_4)_2\text{Ge}^{[6]}[\text{Ge}^{[4]}_6\text{O}_{15}]$ leads us back to Fig. 2(a). In this approach we focus on the donor nature of the $\text{Ge}^{[6]}$ atoms (dark blue spheres), which are connected to the six $\text{Ge}^{[4]}$ atoms (cyan spheres) at distances $\text{Ge}^{[6]}-\text{Ge}^{[4]}$ of $6 \times 3.19 \text{ \AA}$. These groups of seven Ge atoms form blocks that are highlighted when the connections between $\text{Ge}^{[4]}$ atoms of different blocks in Fig. 2(a) are omitted, so giving rise to the pattern represented in Fig. 4(a) where the N atoms have now been drawn as lilac spheres to show how they intercalate between the Ge-clusters.

The most relevant feature of this fragment is that it reproduces *almost completely* the structure of the rutile-like structure of GeO_2 . In fact, the fragment represented in Fig. 5(a) corresponds to two unit cells of GeO_2 (rutile) in which two opposite Ge atoms are missing. This is better understood when we compare this drawing with the real rutile structure of GeO_2 that is represented in Figs. 5(b) and (c).

In Fig. 5(d) the rutile-like fragment is projected onto the hypothetical (001) plane. The central Ge atom (dark blue) is octahedrally coordinated, so sharing the six corners with six GeO_4 tetrahedra as shown in Figs. 5(d), and in turn

mimicking the corner-sharing of the octahedral arrangement found in the real rutile-like structure drawn in Fig. 5(e).

Regarding dimensions, the rutile-like fragments in $\text{NH}_4\text{Ge}^{[6]}[\text{Ge}^{[4]}_6\text{O}_{15}]$ (Fig. 5a) have Ge–Ge distances of $4.23 \times 4.28 \times 3.02 \text{ \AA}$, with six Ge–Ge distances of 3.19 \AA (red lines in Fig. 5a). These values are comparable to those of the unit cell of the rutile-like GeO_2 ($P4_2/mnm$; Fig. 5e), with $a = b = 4.39$, $c = 2.90$, $d = 8 \times 3.42 \text{ \AA}$. These parameters are equivalent to the distances labelled as a and c in Figs. 5(a) and (b) of germanate. The Ge–Ge–Ge angles (86°) deviate slightly from the ideal values (90°) in the tetragonal rutile-like structure (cf. Figs. 5d and e).

If now we consider Fig. 4(a) we see that if the N atoms (lilac spheres) are removed the ‘rutile-like’ Ge_7 blocks collapse to form the structure of GeO_2 . This is more clearly seen in Fig. 4(b) where if the two blocks approach each other a larger fragment of the rutile structure can be obtained.

4. Discussion

From the above structural description, two aspects are evident. Firstly, that the Extended Zintl–Klemm Concept that was previously applied to aluminates and silicates (Santa-

maría-Pérez & Vegas, 2003; Santamaría-Pérez *et al.*, 2005) works equally well for the germanate, despite the lower electronegativity of Ge with respect to Si. This compound provides additional evidence for the possibility of charge transfer between nominal cations – even if they are of the same species – as has been illustrated for the compounds CsLiSO_4 and Na_2SO_4 (Vegas & García-Baonza, 2007). This new way of interpreting the crystal structures has been further emphasized in the works by Vegas (2012) concerning the ternary alkali oxides and chalcogenides, and by Vegas *et al.* (2009) and Vegas (2017) when presenting this novel new interpretation of the stuffed-bixbyites structures.

From the data described above it seems that the achievement of these cation networks, which are intimately related to the structures of p -block elements, is a *fundamental factor* of both the underlying structural and the thermodynamic stability. If the stoichiometry does not allow for the formation of such a network, then some of the atoms act as true cations in order to transform the other similar atoms into the Zintl-polyanions like that of $[\text{Ge}_2\text{O}_5]^{2-}$ as shown in Fig. 2(b).

The second aspect of crucial importance to be outlined in this paper refers to the behaviour of the $\text{Ge}^{[6]}$ atom. At first glance, one might think that its *true cationic character* would

cause it to be regarded as an *isolated entity*. However, as seen above (Fig. 5), its octahedral coordination provokes, to some extent, the extension of a distorted, and so modified, structure of the rutile-like GeO_2 . We have used the expression ‘to some extent’ because at present we are not able to understand exactly the physical reasons for this behaviour. What we can say, however, is that after having dissected this crystal structure, each of the two opposite characters exhibited by the Ge atoms (Ge^{4+} and Ge^-) yield two opposite partial structures, *i.e.* rutile and the Zintl polyanion, respectively.

The important result, however, is that both structures must necessarily become compatible and for this reason the rutile unit cell is completed with tetrahedra at the same time as the ladder-type skeleton of Ψ -As is being spatially modified whilst maintaining its threefold connectivity. Both structures must be satisfied simultaneously as has already been described in our previous articles discussing the stuffed-bixbyites (Vegas *et al.*, 2009) and FeLiPO_4 (Vegas, 2011, 2017). Such an inter-

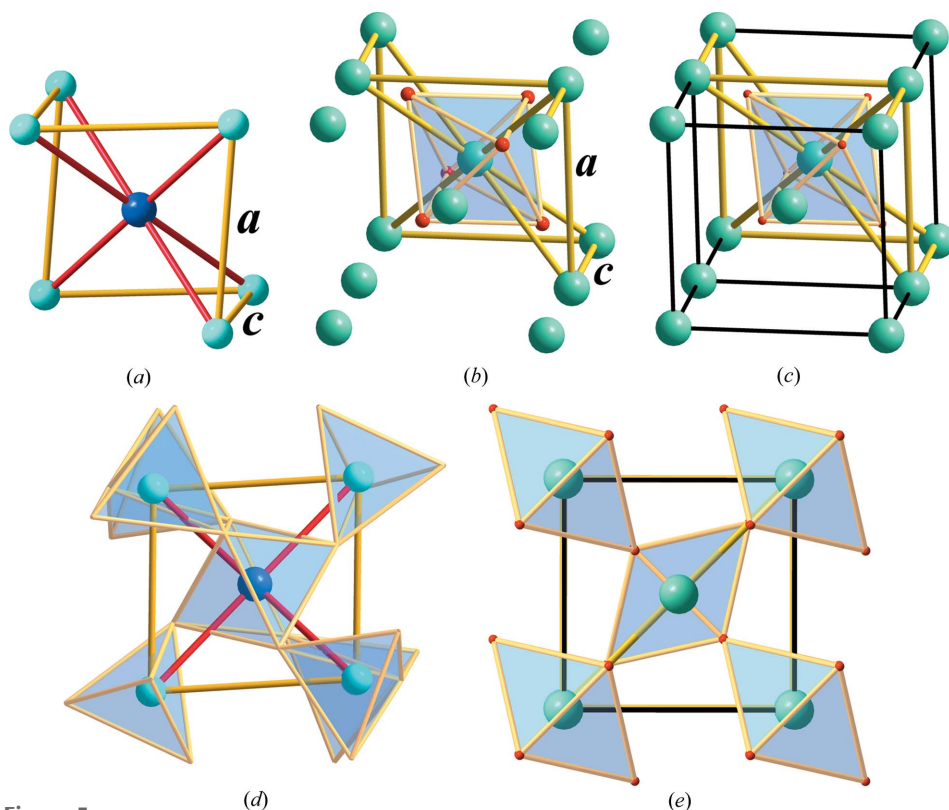


Figure 5

(a) Perspective view of the octahedral $\text{Ge}^{[6]}$ atom (dark blue) connected to the six tetrahedral $\text{Ge}^{[4]}$ atoms (cyan) in a fashion that partially reproduces the structure of the rutile-type GeO_2 represented in (b). (b) Two unit cells of the rutile-type structure of GeO_2 . The unit cell edges have been omitted but the fragment reproduced in (a) has been highlighted with yellow lines, together with the central GeO_6 octahedron. (c) Two unit cells of the rutile-type structure of GeO_2 . The bonds drawn in ochre colour are those forming the corresponding fragment in (b) and in (d). (d) The fragment represented in (a) but projected to show the connectivity of the central octahedron to the six tetrahedra. (e) A projection of the rutile-like structure of GeO_2 to be compared with the fragment in (c) and with the defect structure in (d).

pretation is in accordance with the thermogravimetric analysis–thermal desorption analysis (TGA–TDA) experiments which have been reported (Cascales *et al.*, 1998) on the compound which shows an endothermic process accompanied by a weight loss in the range 593–723 K. This corresponds to the decomposition of $(\text{NH}_4)_2\text{Ge}_7\text{O}_{15}$ by loss of one H_2O and two NH_3 molecules. Powder X-ray diffraction data shows that the structure of Fig. 1(a) is maintained after heating to 585 K but then collapses, at 723 K, to yield GeO_2 .

Thus, the $(\text{NH}_4)_2\text{O}$ -free skeleton (Fig. 2a) is maintained as a metastable structure up to a temperature of 723 K at which point the bonds eliminated when passing from Figs. 4(a) and 5(a) [fragments of $(\text{NH}_4)_2\text{Ge}_7\text{O}_{15}$] to Fig. 5(c) (a rutile-like structure) bring about the underlying collapse of the structure, as the blocks of Fig. 4(a) approach each other to form the rutile GeO_2 of Fig. 5(e).

5. Thermodynamic aspects of the Zintl–Klemm concept

The ionic strength, I , of a lattice is directly proportional to the lattice potential energy, U_{POT} (Jenkins & Glasser, 2000), and hence to the lattice stability. The relationship is represented by the equation

$$U_{\text{POT}} = AI(2I/V_m)^{1/3}, \quad (1)$$

where A is a constant and V_m is the formula unit volume. So transforming one lattice into another one having a higher value of $I^{4/3}$ (which we can simplify to consideration of just the value of I itself) will imply increased stability. There is no change in the formula unit volume V_m because we are merely proposing a rearrangement of the charge within the *same* lattice. From this charge rearrangement we create a more stable pseudo-lattice when compared with the case where we calculate I on the basis of tetravalent Ge in the germanate.

Thus, consideration of $(\text{NH}_4)_2\text{Ge}_7\text{O}_{15}$ as a pseudo-polyanion $\Psi\text{-As}_2\text{O}_5$ (in terms of the Zintl–Klemm concept) should yield a more stable skeleton compared with the originating lattice (as Ge_2O_5). In other words, calculations of I considering Ge as $\Psi\text{-As}$ should produce a more stable lattice than when we calculate I on the basis of tetravalent Ge in the germanate. The ionic strength, I , of a lattice is simply calculated using the formula

$$I = \frac{1}{2} \sum n_i z_i^2, \quad (2)$$

where the summation is performed over the entire lattice and n_i is the number of ions having charge z_i . Thus I for $(\text{NH}_4)_2\text{Ge}_7\text{O}_{15}$ is equal to: $\frac{1}{2}[2 \times 1^2 + 7 \times 4^2 + 15 \times (-2)^2] = \frac{1}{2}[2 + 112 + 60] = 174/2 = 87$ treating the NH_4^+ as a charge of +1, leading to a calculation of I for $3 \times \Psi\text{-As}_2\text{O}_5$ a point = $\frac{1}{2}[3 \times [2 \times 5^2 + 5 \times (-2)^2]] = \frac{1}{2}[3 \times [50 + 20]] = 210/2 = 105$. Thus, the ionic strength (and hence stability) has been increased from 87 to 105 by virtue of the above rearrangement. The stability enhancement ratio is $S = 1.21$ (see Jenkins & Vegas, 2017). As justification of the validity of this new approach developing the theory of pseudo-lattice generation we will show in our next paper (Jenkins & Vegas, 2017) that, in every case, there

always results an increase in the ionic strength, I , on generation of the pseudo-lattice, indicative of an enhanced stability.

6. Concluding remarks

The structure of $(\text{NH}_4)_2\text{Ge}_7\text{O}_{15}$ as discussed in this paper illustrates the fact that the classical description of inorganic structures in terms of cation-centred anionic polyhedral is now outdated, providing, as it does, a poor insight of all the chemical interactions occurring in the crystal. In contrast, the application of the Extended Zintl–Klemm Concept leads to the discovery of interesting new outcomes that arise due to the different role played by atoms of the same species (in this case Ge) as a function of their donor/acceptor character. A comparison of Fig. 1 with Fig. 5 reveals the important structural and chemical aspects that remain hidden in a conventional description but that emerge when the new concept is applied. Thus, a new concept is required and although slow to gain acceptance (as is often the case where new thinking is required) our approach satisfies this need. The approach will be further elucidated in a fuller study in preparation and due for publication in 2017 (Vegas, 2017).

The electrons transferred by the donor NH_4^+ and Ge^{4+} cations to the Ge^- anions account for the threefold connectivity of the $\Psi\text{-P}$ atoms constituting the backbone of the $[\text{Ge}^{[4]}\text{O}_4]$ network. However, at the same time, the donor Ge^{4+} cations strive towards the formation of fragments of its stable GeO_2 structure and hence, the $(\text{NH}_4)_2\text{Ge}_7\text{O}_{15}$ structure rearranges in order to satisfy both structures simultaneously. For the first time, the Extended Zintl–Klemm Concept (EZKC) used so far to explain other similar structures is reinforced here by the application of the thermodynamic ionic strength. This charge transfer assumed by the Extended Zintl–Klemm Concept not only accounts for the structural changes occurring in the $[\text{TO}_4]$ network, but it seems to be the driving force that compels the structure towards its greatest thermodynamic stability as predicted from the respective I values. We believe that this article should be necessary reading for all those concerned with crystal structure arrangements as it represents a new era in the way of understanding the role that atomic species can play.

References

- Bissert, G. & Liebau, F. (1969). *Naturwissenschaften*, **56**, 212.
- Cascales, C., Gutiérrez-Puebla, E., Monge, M. A. & Ruiz-Valero, C. (1998). *Angew. Chem. Int. Ed.* **37**, 129–131.
- Durif, A. (1995). *Crystal Chemistry of Condensed Phosphates*. Heidelberg: Springer.
- Fleet, M. E. (1996). *Am. Mineral.* **81**, 1105–1110.
- Fleet, M. E. (1998). *Am. Mineral.* **83**, 618–624.
- Fleet, M. E. & Henderson, G. S. (1995). *Phys. Chem. Miner.* **22**, 383–386.
- Goldschmidt, V. M. (1932). *Z. Phys. Chem. Abt. B*, **17**, 172–176.
- Jenkins, H. D. B. & Glasser, L. (2000). *J. Am. Chem. Soc.* **122**, 632–638.
- Jenkins, H. D. B., Roobottom, H. K., Passmore, J. & Glasser, L. (1999). *Inorg. Chem.* **38**, 3609–3620.
- Jenkins, H. D. B. & Vegas, A. (2017). In preparation.

- Köllisch, K. & Schnick, W. (1999). *Angew. Chem. Int. Ed.* **38**, 357–359.
- Liebau, F. (1985). *Structural Chemistry of Silicates. Structure, Bonding and Classification*. Berlin: Springer.
- Parthé, E. & Chabot, B. (1990). *Acta Cryst.* **B46**, 7–23.
- Parthé, E. & Engel, N. (1986). *Acta Cryst.* **B42**, 538–544.
- Poojary, D. M., Borade, R. B. & Clearfield, A. (1993). *Inorg. Chim. Acta*, **208**, 23–29.
- Santamaría-Pérez, D. & Vegas, A. (2003). *Acta Cryst.* **B59**, 305–323.
- Santamaría-Pérez, D., Vegas, A. & Liebau, F. (2005). *Struct. Bond.* **118**, 121–177.
- Stishov, S. M. & Belov, N. V. (1962). *Dokl. Akad. Nauk SSSR*, **143**, 951–954.
- Svensson, C. (1974). *Acta Cryst.* **B30**, 458–461.
- Swanson, D. K. & Prewitt, C. T. (1983). *Am. Mineral.* **68**, 581–585.
- Vegas, A. (2011). *Struct. Bond.* **138**, 67–91.
- Vegas, A. (2012). *Acta Cryst.* **B68**, 364–377.
- Vegas, A. (2017). *New Models in Inorganic Structures*. Oxford University Press. In preparation.
- Vegas, A. & García-Baonza, V. (2007). *Acta Cryst.* **B63**, 339–345.
- Vegas, A., Martin, R. L. & Bevan, D. J. M. (2009). *Acta Cryst.* **B65**, 11–21.
- Yang, H., Hazen, R. M., Finger, L. W., Prewitt, C. T. & Downs, R. T. (1997). *Phys. Chem. Miner.* **25**, 39–47.